



Comparative dehydrogenation of cyclohexanol to cyclohexanone with commercial copper catalysts: Catalytic activity and impurities formed

Arturo Romero^{a,*}, Aurora Santos^a, Daniel Escrib^b, Ernesto Simón^a

^a Departamento de Ingeniería Química, Facultad de Químicas, Universidad Complutense de Madrid, Ciudad Universitaria, 28040 Madrid, Spain

^b UBE Corporation Europa S.A., Polígono Industrial El Serrallo s/n, 12100 Castellón, Spain

ARTICLE INFO

Article history:

Received 27 July 2010

Received in revised form 4 October 2010

Accepted 18 October 2010

Available online 12 November 2010

Keywords:

Alumina

Catalyst

Chromium

Copper

Cyclohexanol

Cyclohexene Cyclohexanone

Dehydrogenation

Phenol

Zinc

ABSTRACT

Catalytic dehydrogenation of cyclohexanol to cyclohexanone has been carried out on phase gas in a continuous fixed bed reactor under atmospheric pressure. Copper chromite and copper zinc oxide catalysts have been checked. Effect of temperature (in the range 250–290 °C) and spatial time in reactor have been studied. The catalytic activity has been evaluated in terms of cyclohexanone yields and impurities from secondary reactions of dehydration and dehydrogenation of cyclohexanol have also been identified and quantified by GC/MS.

Catalysts have been characterized by X-ray diffraction, temperature programmed desorption of ammonia and BET surface area measurement. High activity was confirmed by copper-based catalysts under the operating conditions, concerning the size and dispersion of the copper specie. It was also found that catalysts with alumina and chromium exhibit higher dehydration capacity, being cyclohexene the main impurity obtained. For a given cyclohexanone yield the impurities from dehydrogenation reactions showed similar trends for the three catalysts tested. Phenol was the main impurity obtained by dehydrogenation.

© 2010 Elsevier B.V. All rights reserved.

Nomenclature

d_p	particle diameter (mm)
ρ_p	particle density (g cm^{-3})
ρ_L	bed density (g cm^{-3})
S_{BET}	BET surface area ($\text{m}^2 \text{g}^{-1}$)
V_p	pore volume ($\text{cm}^3 \text{g}^{-1}$)
WHSV	weight hourly space velocity (h^{-1})
Y_{ONE}	cyclohexanone percentage yield (%)
Y_j	impurity j percentage yield (%)
$Y_{\text{H}_2\text{O}}$	water percentage yield (%)
Y_{H_2}	total yield of hydrogen (%)
$Y_{\text{H}_2 \text{ imp}}$	hydrogen yield from impurities (%)
$S_{\text{H}_2 \text{ imp}}$	selectivity to hydrogen from impurities

1. Introduction

Catalytic dehydrogenation of cyclohexanol to produce cyclohexanone is an important industrial process especially in producing

ϵ -caprolactam, main raw material in the manufacture of nylon-6. As a polyamide fiber raw material must increasingly fulfill meet higher purity requirements [1]. The impurities can come from the products formed in the transformation stages of the reagents as dehydrogenation of cyclohexanol, which is a critical process, where is necessary to minimize the impurities that affect seriously the later stages. From an industrial point of view, the heterogeneous catalytic gas-phase dehydrogenation at atmospheric pressure is severely restricted by highly endothermic reaction ($\Delta H = 65 \text{ kJ/mol}$) and thermodynamic equilibrium [2], and also includes a complex consequent-parallel reactions, where cyclohexanone selectivity decreases because of an increase of the impurities yields [3,4].

There are two methods for dehydrogenation of cyclohexanol, at low temperature, from 200 to 300 °C, and at high temperature, from 350 to 450 °C. Copper oxide based catalyst is usually used at low temperature [4–18]. Metals such as Zn, Cr, Fe, Ni, alkali metals, alkaline earth metals, and thermally stable metal oxides (Al, Si, and Ti) are added. Chromia acts as a structural promoter because it increases the BET surface area and also inhibits the sintering of copper particles [19]. Zinc calcium oxide has been used at high temperature. Copper catalysts are not used at high temperature to avoid sintering of the copper [20].

In the recent years, more attention has been paid in literature to these low temperature catalysts compared to high temperature.

* Corresponding author. Tel.: +34 913944171; fax: +34 913944171.

E-mail address: aromeros@quim.ucm.es (A. Romero).

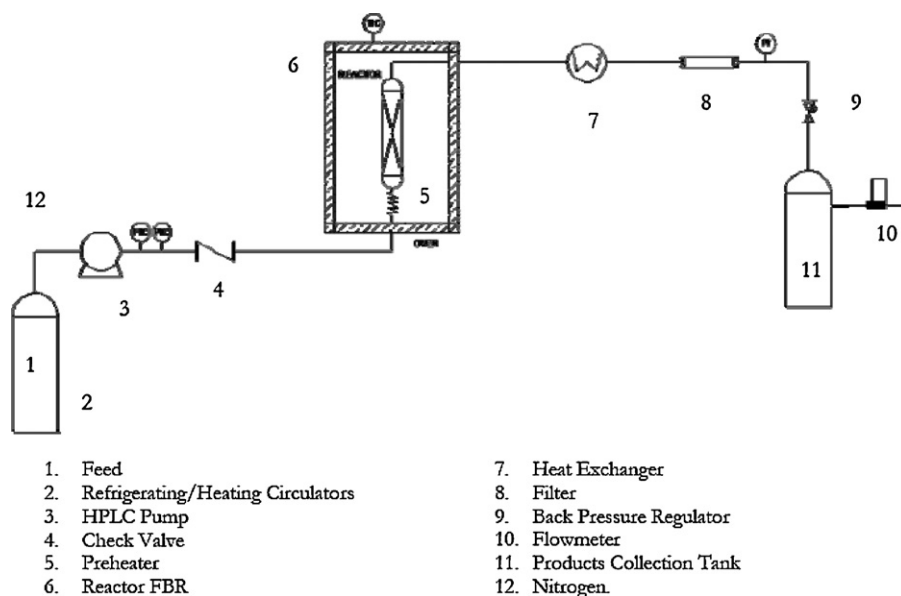


Fig. 1. Experimental setup for cyclohexanol dehydrogenation.

Cesar et al. [9] used a bimetallic catalyst adding Co to Cu/SiO₂ and a commercial Cu/SiO₂ catalyst. Fridman and Davydov [10] tested a Cu/Mg, Cu/Zn and Cu/Zn/Al catalysts. Siva Kumar et al. [14] examined a Cu/ZnO based catalysts promoted with Cr₂O₃ and La₂O₃–Cr₂O₃ as double promoter. Ji et al. [15] used a Cu/SiO₂ and Cu–ZnO/SiO₂ catalysts. Nagaraja et al. [16,17] tested a Cu/MgO catalyst, Cu–Cr₂O₃/MgO promoted catalyst and a commercial Cu-1800P catalyst.

Many researchers have analyzed the influence of the support, the preparation method and copper loading on both the activity and selectivity to cyclohexanone of different copper-containing catalysts, to increase the conversion of cyclohexanol to cyclohexanone. In these works, both cyclohexanol conversion and cyclohexanone yield data are well documented. However, to our best knowledge, few results about the impurities and their corresponding yields can be found. Cyclohexene from cyclohexanol dehydration and phenol from cyclohexanol dehydrogenation are in general the impurities identified by authors [4,7,15].

The present study was carried out to evaluate the performance of copper chromite and copper zinc oxide catalysts for dehydrogenation of cyclohexanol at different temperatures and spatial times in reactor. The catalytic activity was studied in terms of cyclohexanone yield. Moreover, the main dehydration and dehydrogenation impurities from cyclohexanol were identified and quantified by GC/MS. Results obtained for activity and selectivity were also discussed attending the catalyst properties.

2. Experimental

2.1. Chemicals and catalysts

Cyclohexanol (Sigma–Aldrich, 105899), cyclohexanone (Fluka, 29135), benzene (Fluka, 12540), cyclohexene (Aldrich, 24,099-0), phenol (Riedel-de Haën, 33517), 2-cyclohexen-1-one (Fluka, 29255), 2-cyclohexylidene-cyclohexanone (Alfa-Aesar, L09798) and 1,4-benzodioxan (Aldrich 179000) have been used as reactants or standards. Three commercial catalysts have been employed. Copper chromite catalysts, Cu-1230 (crushed, 1.7 × 4.7 mm) and Cu-0203 (tablets, 3.1 × 3 mm), were supplied by Engelhard, and copper zinc oxide catalyst, T-2130 (tablets, 3 × 3 mm), was provided by Süd-Chemie.

2.2. Catalytic activity

Catalytic dehydrogenation of cyclohexanol to cyclohexanone on gas phase was carried out at atmospheric pressure in a continuous flow fixed-bed reactor made of a stainless-steel tube with 0.85 cm internal diameter and 25 cm length. The bed was filled with 10 g of each catalyst. The bed volume was completed with nonporous glass spheres, inert glass wool and stainless-steel wire mesh. As pretreatment the catalysts were reduced with 95% nitrogen 5% hydrogen at 180 °C for 18 h (GHSV = 1100 h⁻¹). A detailed scheme of the experimental setup is given in Fig. 1.

The temperature reactions were 250 and 290 °C. Before the start of the reaction the catalyst was stabilized with N₂ at temperature reaction. Once the reaction is finished, the catalyst was flushed one hour in N₂ flow and later was also cooled at room temperature in nitrogen atmosphere. Cyclohexanol was fed with 5 wt.% cyclohexanone to avoid the cyclohexanol solidification (mp 22 °C). The addition of cyclohexanone in the raw material does not affect the results of impurities obtained. Feed was pumped through high precision pump. The liquid flow rate was changed from 0.1 to 1 mL min⁻¹ (WHSV from 0.43 to 5.80 h⁻¹). The vapour effluent from the reactor was cooled at 20 °C and liquid and gas phase were separated and collected, and liquid phase was analyzed by chromatography. The catalysts were run for 6 h under operations conditions for each experiment. After 2 h of reaction, the steady state was achieved. No changes in catalyst activity during this period of time were observed. The steady state samples were analyzed and these values were used for all subsequent calculations. We have confirmed the absence of external and internal mass transport resistances by changing particle diameter and superficial velocity. Moreover, pressure drop in fixed bed was negligible.

2.3. Catalysts characterization

BET surface area and pore volume were determined using N₂ adsorption method at liquid nitrogen temperature (77 K) on a Beckman Coulter SA3100 Analyzer. Before each measurement, the sample was degassed at 563 K for 60 min.

XRD patterns were recorded on a Philips X'Pert diffractometer, using monochromated Cu K α radiation ($\lambda = 1.5418 \text{ \AA}$), operating at 45 kV and 40 mA. The measurements were recorded in steps of 0.04° with a count time of 1 seg. in the 2 Theta range of 5–90°.

The acidity was determined by NH₃-TPD. Before the adsorption of ammonia, the samples were treated under helium at 500 °C (from 25 to 500 °C in 20 min.) for 1 h. The samples were then cooled at 100 °C in He flow, and then treated with a NH₃ flow for 5 min at 100 °C. The physisorbed ammonia was eliminated by flowing He for 1 h at 300 °C. The NH₃-TPD was run between 100 and 500 °C at 10 °C/min and followed by an on-line gas chromatograph, GC-15A from Shimadzu, provided with a thermal conductivity detector.

2.4. Analytical methods

Cyclohexanol and cyclohexanone were analyzed by GC/FID (HP 6890 GC-FID). Impurities of the cyclohexanol dehydrogenation were analyzed by GC/MS (HP 6890N GC MSD 5975B). For both analysis a HP-INNOWAX 19091N- 133 (crosslinked PEG) 30 m × 0.25 mm \varnothing_1 × 0.25 μ m column were used. 1,4-benzodioxan was used as ISTD for calibration.

Standards used for quantitative analysis were calibrated from their commercial products. The impurities identified not available as commercial products (2-cyclohexyl-cyclohexanone, 2-cyclohexylidene-cyclohexanol and 2-cyclohexyl-cyclohexanol) were assigned to the response of 2-cyclohexylidene-cyclohexanone.

3. Results and discussion

3.1. Catalysts characterization

Table 1 summarizes the physico-chemical properties of the reduced catalysts. As can be observed, C1 catalyst presents major BET surface area due to the presence of alumina in its composition. In C2 and C3 catalysts the BET surface area are provided by copper chromite and zinc oxide, respectively [19].

The NH₃-TPD profiles and the deconvolution of the NH₃-TPD curves for reduced catalysts are shown in Fig. 2. The area under these curves is the total amount of NH₃ desorbed over the range of temperature. Based on the desorption temperature, the acid sites can be classified as weak (150–250 °C), medium (250–350 °C) and strong (350–450 °C) [27]. The acidity depending on their strengths is reported in Table 1. C1 catalyst presents highest amount of moderate acid sites and a significant amount of strong acid sites. These acid sites show C1 catalyst as the most acidic, also due to alumina. C2 and C3 catalysts do not exhibit acidity.

The XRD patterns of the calcined and reduced catalysts of C1, C2 and C3 are shown in Fig. 3. The copper crystallite size was estimated from Debye–Scherrer equation from the XRD patterns of the reduced catalysts. These data are also summarizes in Table 1.

C1 catalyst. The XRD results of the calcined and reduced catalysts show that C1 is an amorphous catalyst where the intensity of crystalline phases is very low. The calcined catalyst presents peaks corresponding to chromate and chromite. In the calcined catalyst CuO is in the amorphous phase. After reduction the peaks of Cu⁺ and Cu⁰ species appear and the chromate and chromite ones disappear. Some authors have observed that when the Cr content is high (44 wt.% in the form of copper chromite for C1), copper species in XRD are found as copper (I) oxide and metallic copper, and Cr containing species cannot be seen by XRD, which suggests that the copper species are highly dispersed and exists in amorphous phase [14,21]. In the reduced catalyst, Cu₂O and Cu⁰ crystallites size are distinguished. The size of Cu₂O is minor than Cu⁰.

C2 catalyst. The XRD patterns indicate that after reduction in an atmosphere of hydrogen, the peaks of CuO disappear and the peaks of Cu⁰ appear. In the calcined catalyst the CuCr₂O₄ specie is hardly distinguished and is maintained in reduced catalyst. Some authors observed that copper chromite is not reduced in an atmosphere

Table 1
Physico-chemical properties of reduced catalysts.

Commercial catalyst	Composition, wt. %	Cu, wt. %	Physical and chemical properties					Acidity, μ mol NH ₃ g ⁻¹			Phases XRD		Cu crystallite size, nm	
			d_p mm	ρ_p g cm ⁻³	ρ_s g cm ⁻³	S_{BET} , m ² g ⁻¹	V_p , cm ³ g ⁻¹	Weak	Moderate	Strong	Total	Reduced	Reduced	Reduced
C1 Cu-1230 Engelhard	CuO,15 CuCr ₂ O ₄ ,44 BaCrO ₄ ,12 Al ₂ O ₃ ,29	24	1.6	1.50	1.17	121.8	0.300	38	206	74	318	Cu Cu ₂ O	Cu Cu ₂ O	15.5 8.8*
			3.17	3.33	2.20	13.5	0.040	4	14	2	20	Cu CuCr ₂ O ₄ C graphite	Cu CuCr ₂ O ₄ C graphite	27.2
C2 Cu-0203 Engelhard	CuCr ₂ O ₄ ,26 C graphite,2 CuO,33	26	3	2.30	1.76	43.4	0.223	3	27	0	30	ZnO C graphite	ZnO C graphite	9
			T-2130 SüdChemie											

* Corresponding to Cu₂O phase.

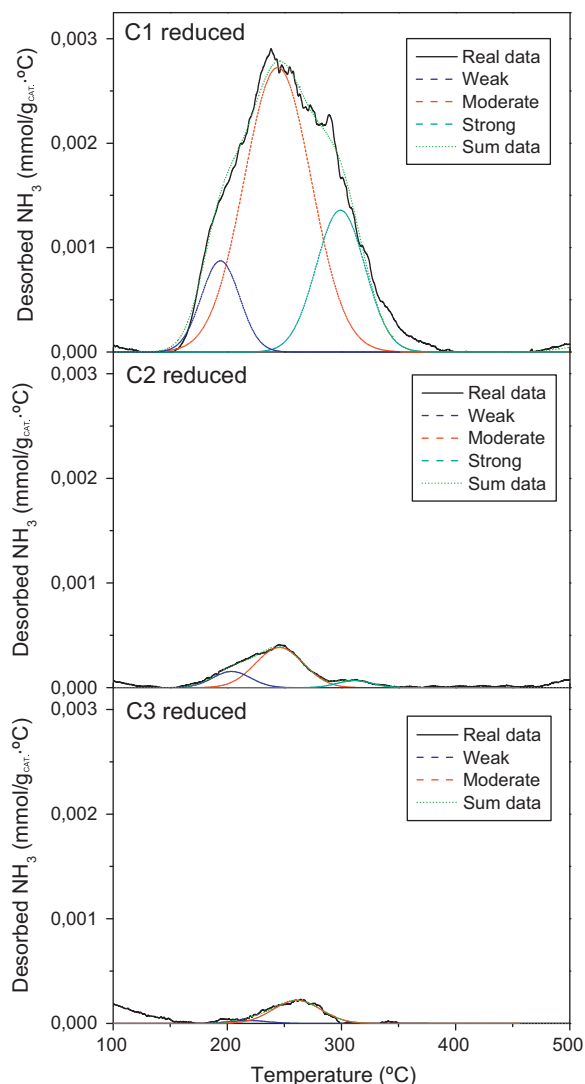


Fig. 2. NH₃-TPD patterns and deconvoluted NH₃-TPD curves for reduced catalysts of C1, C2 and C3.

of hydrogen [19,22]. Cu⁰ crystallite size of C2 is a higher than Cu⁰ and Cu₂O crystallite sizes in C1. Minor BET surface area and major Cu content (65 wt.%) suggests that C2 catalyst presents lower Cu dispersion.

C3 catalyst. The XRD data of the calcined and reduced catalyst indicate that CuO is transformed into Cu⁰. The XRD profile of zinc oxide has not been affected by reduction. The low intensity of the CuO specie diffraction peaks may suggests that the copper is highly dispersed in the zinc oxide phase [23,24]. For C3 catalyst, the Cu⁰ crystallite size is smaller than that in C1 and C2 but in the same order of magnitude as Cu₂O of the C1 catalyst. Presence of smaller Cu⁰ crystallite size, major BET surface area and minor Cu content than C2, are a clear indication of higher copper dispersion in C3 catalyst.

3.2. Catalytic activity

The main impurities generated in dehydrogenation of cyclohexanol to cyclohexanone at 250 and 290 °C with C1, C2 and C3 catalysts have been identified and quantified by GC/MS. These impurities (acronyms, formula, weight molecular, CAS number and molecular structure) are given in Table 2. It is noted that these impurities are obtained from dehydration (CXEN, BZN, CXCXONA,

CXCXOL, CXECXONE and CXECXOL) and dehydrogenation reactions (CXENONE, PHOH and BZN). Benzene has been associated to both processes, as it may be obtained as the result of dehydration and further dehydrogenation of cyclohexanol. In order to confirm the assignments of the identified compounds the MS library standards of these compounds have been analyzed and used for calibration. The coincidence of retention time and spectrum between the standards and the run products allows validating the assignments done. The impurities identified not available as commercial products (2-cyclohexyl-cyclohexanone, 2-cyclohexylidene-cyclohexanol and 2-cyclohexyl-cyclohexanol) were assigned to the response of 2-cyclohexylidene-cyclohexanone. Spectrum of the peaks associated to these impurities match spectrum of these compounds on the MS library NIST 5.0 with a quality higher than 95%.

From the composition of liquid samples at the collection tank, after separating hydrogen, the molar flows of cyclohexanone, F_{ONE} , and impurities, F_j , are determined, as mol h⁻¹. Cyclohexanone percentage yield, Y_{ONE} , is defined as:

$$Y_{\text{ONE}} = \frac{F_{\text{ONE}} - F_{\text{ONEo}}}{F_{\text{OLO}}} \times 100 \quad (1)$$

The catalytic activity for C1, C2 and C3 catalysts is presented in Fig. 4 as cyclohexanone percentage yield vs. weight hourly space velocity, WHSV, at both temperatures 250 and 290 °C. As can be seen, the catalyst C3 presents higher cyclohexanone percentage yield at both temperatures tested, being even better behavior at 290 °C especially at low weight hourly space velocity (WHSV). The major catalytic activity of C3 could be ascribed to smaller Cu crystallite size and higher dispersion, as reported several authors for Cu–Zn catalysts [6,14,16,18].

It is also observed at these low values of WHSV that as the reaction approaches at equilibrium, cyclohexanone percentage yield does not further increase, and even shows a maximum beyond which starts down the cyclohexanone formed, suggesting that undesirable reactions from cyclohexanone are taking place. Calculated equilibrium conversion for cyclohexanol dehydrogenation to cyclohexanone, at the conditions employed, were about 70% at 250 °C and 80% at 290 °C.

The percentage yield for an impurity j is calculated as the ratio of molar flow of impurity j to the molar flow of cyclohexanol fed to the reactor, and is given as percentage:

$$Y_j = \frac{F_j}{F_{\text{OLO}}} \times 100, \quad j \neq \text{ONE} \quad (2)$$

It was found that the mass balance of cyclohexanol reacted fits quite adequately with the cyclohexanone formed and the impurities obtained.

Results obtained for impurities from dehydration and dehydrogenation reactions are detailed below.

3.3. Impurities from dehydration reactions

Water is directly formed by both dehydration from cyclohexanol to cyclohexene and condensation among six carbon cycles. In this last way, 2-cyclohexylidene-cyclohexanone (CXECXONE), 2-cyclohexyl-cyclohexanone (CXCXONE), 2-cyclohexylidene-cyclohexanol (CXECXOL) and 2-cyclohexyl-cyclohexanol (CXCXOL) are formed.

Molar flow of water to molar flow of cyclohexanol fed to the reactor ratio, denominated molar water yield, $Y_{\text{H}_2\text{O}}$, is calculated from dehydration impurities by stoichiometry, as follows:

$$Y_{\text{H}_2\text{O}} = \frac{F_{\text{H}_2\text{O}}}{F_{\text{OLO}}} \times 100 \cong Y_{\text{CXEN}} + Y_{\text{CXCXOL}} + Y_{\text{CXCXONE}} + Y_{\text{CXECXOL}} + Y_{\text{CXECXONE}} + Y_{\text{BZN}} \quad (3)$$

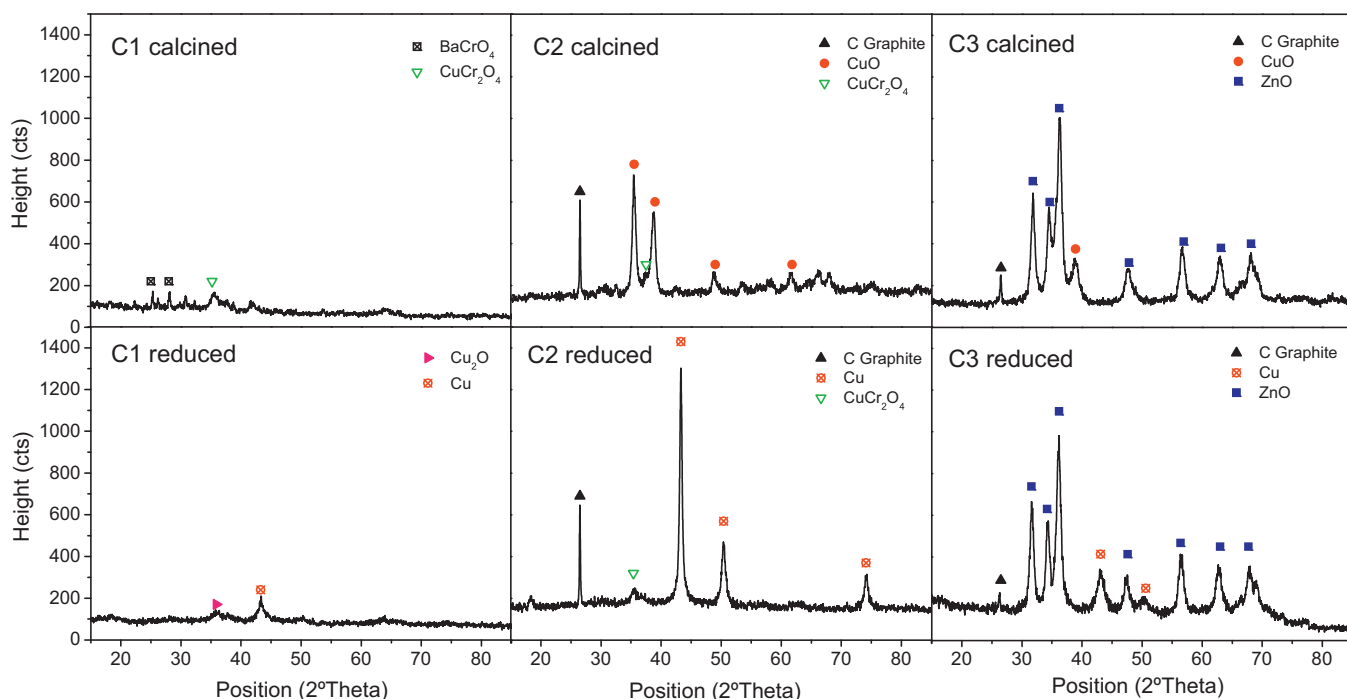


Fig. 3. XRD patterns of calcined and reduced catalysts of C1, C2 and C3.

In Fig. 5 water percentage yield vs. cyclohexanone percentage yield for each catalyst and temperature tested is shown. As can be seen the dehydration reactions are highly favored by C1 catalyst. These results for C1 are in accordance with the aforementioned NH_3 -TPD results. The dehydrating effects of alumina in the compo-

sition of dehydrogenation catalysts have already been described in literature [4,7,25,26]. In C2 catalyst the amount of formed water is also remarkable. Nagaraja et al. [17] found that the largest amount of chrome (44% by weight in the form of copper chromite for C1 catalyst, and 26% for C2) in copper chromite catalysts induces dehydrating effects. From Fig. 5 it can be noticed the great influ-

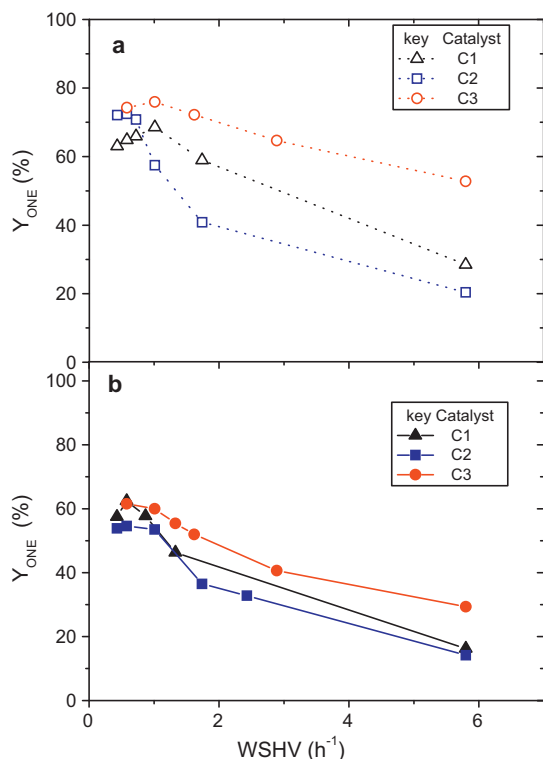


Fig. 4. Cyclohexanone percentage yield as a function of WHSV for each catalyst and temperature tested, (a) 290 °C and (b) 250 °C.

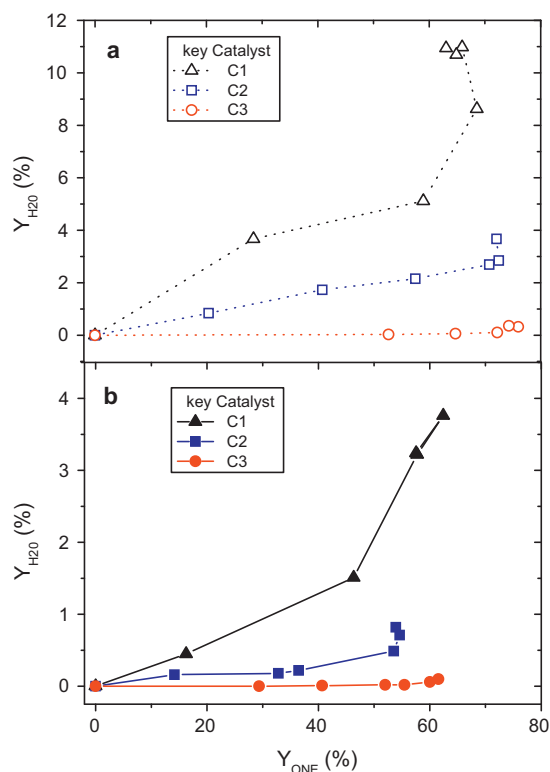
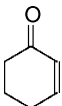
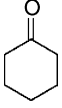
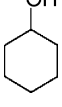
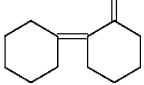
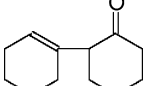
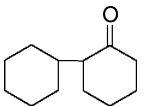
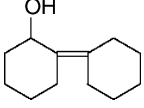
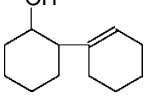
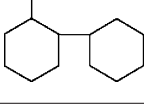


Fig. 5. Water percentage yield as function of cyclohexanone percentage yield for each catalyst and temperature tested, (a) 290 °C and (b) 250 °C.

Table 2
Detected and quantified impurities.

Compound	Acronym	Formula	MW	CAS#	Molecular structure
Benzene	BZN	C ₆ H ₆	78	71-43-2	
Cyclohexene	CXEN	C ₆ H ₁₀	82	110-83-8	
Phenol	PhOH	C ₆ H ₆ O	94	108-95-2	
2-Cyclohexen-1-one	CXENONE	C ₆ H ₈ O	96	930-68-7	
Cyclohexanone	ONE	C ₆ H ₁₀ O	98	108-94-1	
Cyclohexanol	OL	C ₆ H ₁₂ O	100	108-93-0	
2-Cyclohexylidene-cyclohexanone				1011-12-7	
	CXEXONE	C ₁₂ H ₁₈ O	178		
2-(1-Cyclohexenyl) cyclohexanone				1502-22-3	
2-Cyclohexyl-cyclohexanone	CXCXONE	C ₁₂ H ₂₀ O	180	90-42-6	
2-Cyclohexylidene-cyclohexanol				100314-24-7	
	CXEXCOL	C ₁₂ H ₂₀ O	180		
2-(1-Cyclohexenyl) cyclohexanol				66500-79-6	
2-Cyclohexyl-cyclohexanol	CXCXOL	C ₁₂ H ₂₂ O	182	6531-86-8	

ence of temperature on the dehydration yield. Water production rises when temperature increases. As expected, this effect is more remarkable for C1 and C2.

In Figs. 6–9 profiles of main impurities from dehydration reaction at 250 and 290 °C are shown. Cyclohexene yield is shown in Fig. 6, sum of 2-cyclohexylidene-cyclohexanone and 2-cyclohexyl-cyclohexanone yield is given in Fig. 7, sum of 2-cyclohexylidene-cyclohexanol and 2-cyclohexyl-cyclohexanol yield in Fig. 8 and benzene yield in Fig. 9 yield values are given as molar percentages.

As compared with the results in Figs. 5 and 6 it is deduced that the main impurity from dehydration reactions for C1 and

C2 catalysts is cyclohexene. A significant rate of formation of this impurity is obtained at low cyclohexanone yield and consequently high cyclohexanol concentration (highest values of WHSV). Therefore, it is assumed, as it usually done in literature, that cyclohexene is directly formed from cyclohexanol dehydration. Influence of temperature on cyclohexene yield is similar to the observed one for water yield. The amount of cyclohexene produced in C3 catalyst is almost negligible at both temperatures.

Sum of CXEXONE and CXCXONE shows a similar trend to that observed for cyclohexene. Rate of formation of both impurities is negligible at low cyclohexanone yield (medium rich in cyclohex-

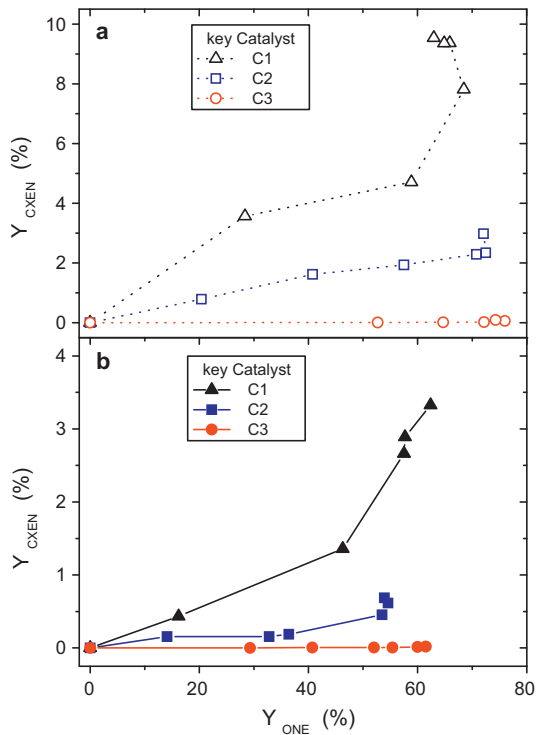


Fig. 6. Cyclohexene percentage yield as a function of cyclohexanone percentage yield for each catalyst and temperature tested, (a) 290 °C and (b) 250 °C.

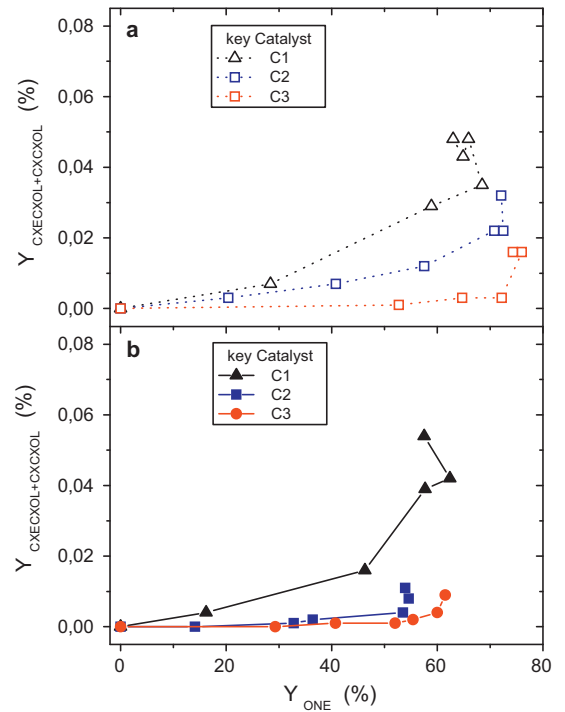


Fig. 8. Sum of 2-cyclohexylidene-cyclohexanol and 2-cyclohexyl-cyclohexanol percentage yield as a function of cyclohexanone percentage yield for each catalyst and temperature tested, (a) 290 °C and (b) 250 °C.

anol). Therefore, it is assumed that these are produced mainly from cyclohexanone. Consequently, the yield for this lumping specie is higher in C1 than in C2 while C3 shows the lower amount for the three catalysts considered. It is also noticed an increase on the

amount of these impurities as temperature rises, being this effect more remarkable in C1 and C2. The higher acidity due to the large amount of acid sites on alumina for C1 catalyst explains the highest activity on dehydration reactions.

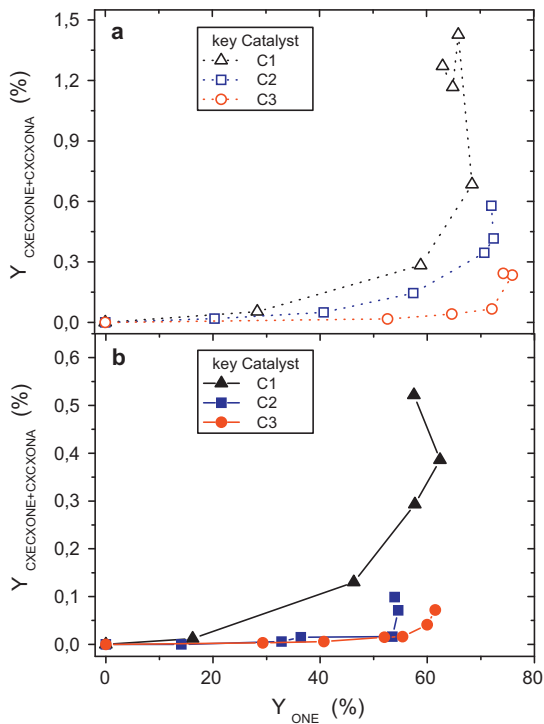


Fig. 7. Sum of 2-cyclohexylidene-cyclohexanone and 2-cyclohexyl-cyclohexanone percentage yield as a function of cyclohexanone percentage yield for each catalyst and temperature tested, (a) 290 °C and (b) 250 °C.

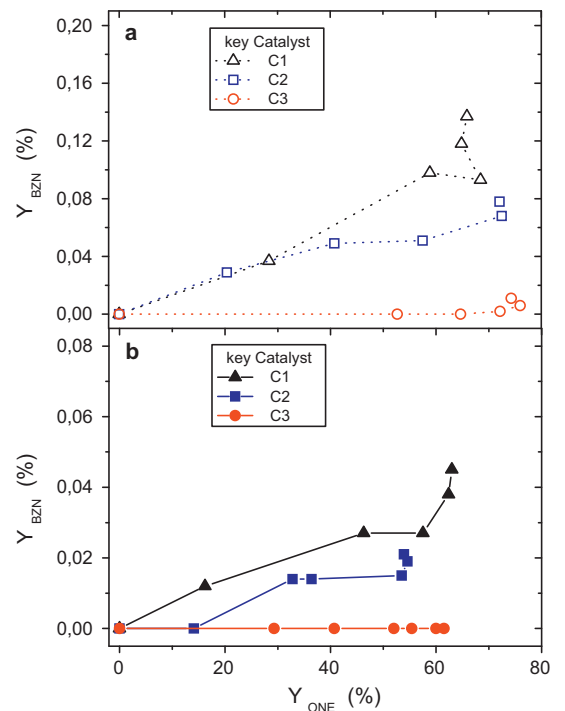


Fig. 9. Benzene percentage yield as a function of cyclohexanone percentage yield for each catalyst and temperature tested, (a) 290 °C and (b) 250 °C.

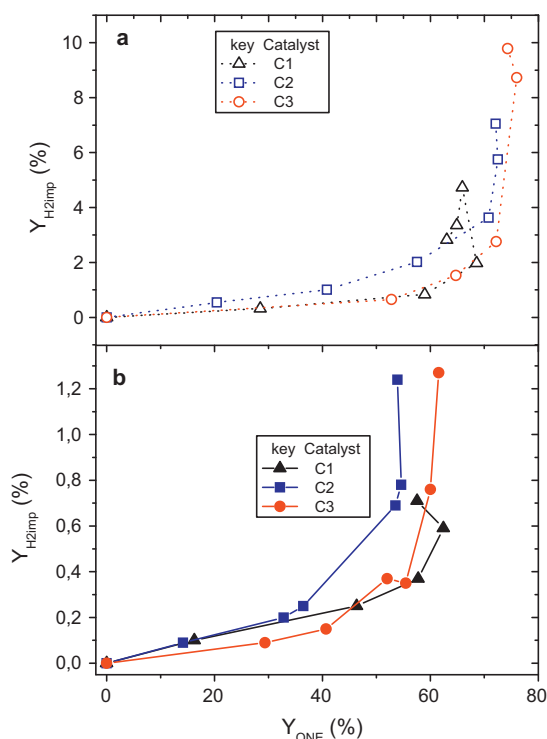


Fig. 10. Hydrogen percentage yield from impurities as a function of cyclohexanone percentage yield for each catalyst and temperature tested, (a) 290 °C and (b) 250 °C.

The sum of CXEXOL and CXCXOL yield, shown in Fig. 8, is always much lower than that corresponding to CXEXONE and CXCXONE but following a similar trend. Rate of formation of both impurities is lower at low cyclohexanone yield (medium rich in cyclohexanol) but the slope is higher than observed for the sum of CXEXONE and CXCXONE. Therefore, it is assumed that the lumped sum of CXEXOL and CXCXOL is produced from condensation of cyclohexanone and cyclohexanol.

A remarkable finding is that significant amounts of cyclohexene (Fig. 6) are obtained from low cyclohexanone yields (media rich in cyclohexanol) but the profiles of condensation impurities in Figs. 7 and 8 are growing exponentially as the reaction approaches at equilibrium (media rich in cyclohexanone).

Benzene yield is shown in Fig. 9. This impurity could be obtained from cyclohexanol dehydration followed by dehydrogenation, in agreement with that previously proposed in literature [7]. In fact, benzene profile agrees with the cyclohexene one in Fig. 6. On the other hand, the amount of this impurity formed in C1 and C2 is two orders of magnitude lower than the corresponding cyclohexene produced. Again, as temperature increases the yield of the impurity rises.

3.4. Impurities from dehydrogenation reactions

By stoichiometry a total yield of hydrogen, Y_{H_2} , defined as the molar flow of hydrogen to molar flow of cyclohexanol fed to the reactor ratio, is calculated. Hydrogen yield from impurities, $Y_{H_2 \text{ imp}}$, which excludes the cyclohexanone produced, has been also obtained. These hydrogen yields are given as percentages and defined by the following expressions:

$$Y_{H_2} = \frac{F_{H_2}}{F_{\text{OLo}}} \times 100 = Y_{\text{ONE}} + 2 \times Y_{\text{CXENONE}} + 3 \times Y_{\text{PhOH}} + 2 \times Y_{\text{BZN}} \quad (4)$$

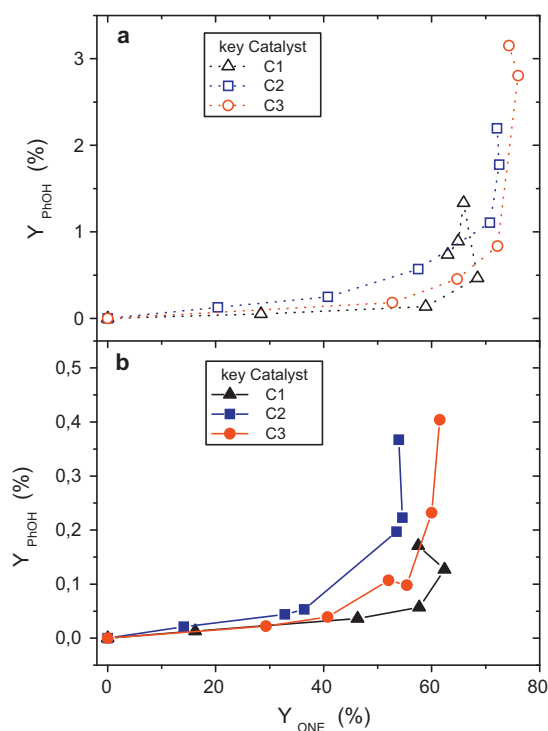


Fig. 11. Phenol percentage yield as a function of cyclohexanone percentage yield for each catalyst and temperature tested, (a) 290 °C and (b) 250 °C.

$$Y_{H_2 \text{ imp}} = \frac{F_{H_2 \text{ imp}}}{F_{\text{OLo}}} \times 100 = 2 \times Y_{\text{CXENONE}} + 3 \times Y_{\text{PhOH}} + 2 \times Y_{\text{BZN}} \quad (5)$$

The values obtained of hydrogen yield from impurities vs. cyclohexanone yield are shown in Fig. 10, for the three catalysts and

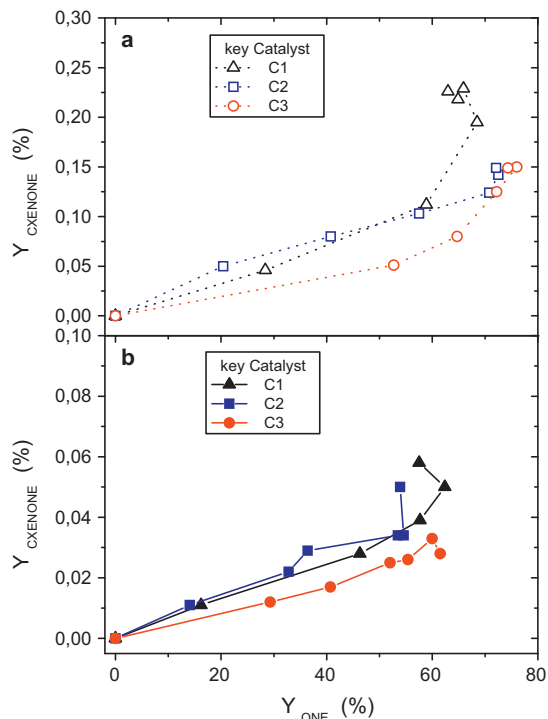


Fig. 12. 2-Cyclohexen-1-one percentage yield as a function of cyclohexanone percentage yield for each catalyst and temperature tested, (a) 290 °C and (b) 250 °C.

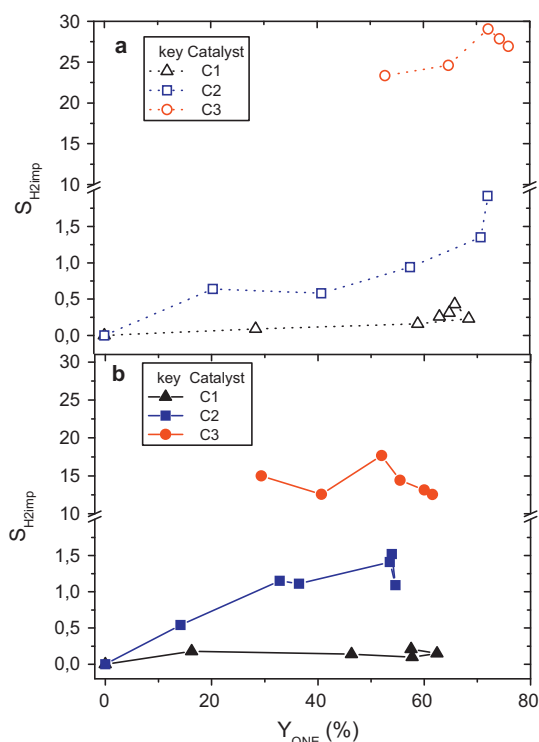


Fig. 13. Selectivity to hydrogen from impurities as a function of cyclohexanone percentage yield for each catalyst and temperature tested, (a) 290 °C and (b) 250 °C.

both temperature tested. As can be seen in this figure, the profile of hydrogen from impurities is similar for the three catalysts. Moreover, formation of hydrogen is quite low at low cyclohexanone yield and increases exponentially as the reaction approaches at equilibrium. At these last conditions the media is rich in cyclohexanone with lower concentration of cyclohexanol. As temperature increases also the hydrogen produced due to formation of impurities does.

In Figs. 11 and 12 are shown phenol and 2-cyclohexen-1-one yields, respectively, as percentage, vs. cyclohexanone yield. These are the main impurities from dehydrogenation reactions found in this work. Benzene yield was already shown in Fig. 9.

As can be observed in Figs. 11 and 12 the profiles of impurities PhOH and 2-CXENONE are quite similar for the three catalysts. Therefore, from these results in Figs. 11 and 12, it can be inferred that no differences can be noticed for both copper sites, Cu^+ and Cu^0 , on dehydrogenation activity.

Phenol is the most important impurity from dehydrogenation and a slightly major amount is generated by the C3 catalyst. Besides, phenol amount produced is quite low at low cyclohexanone yield but increases exponentially as the reaction approaches at equilibrium (media rich in cyclohexanone). Rate of formation of phenol is negligible at low cyclohexanone yield (medium rich in cyclohexanol). Therefore, it is assumed that phenol is produced mainly from cyclohexanone, being this a remarkable finding. Selectivity to hydrogen from impurities is obtained as:

$$S_{H_2 imp} = \frac{Y_{H_2 imp}}{Y_{H_2O}} \quad (6)$$

values obtained for $S_{H_2 imp}$ vs. cyclohexanone percentage yield are shown in Fig. 13 for each catalyst and temperature tested. As can

be seen in Fig. 13 higher hydrogen selectivity increases as follows $C3 > C2 > C1$, being this in agreement with the dehydration capacity obtained for these catalysts.

4. Conclusions

Impurities from dehydration reactions were due to the presence of alumina or chromium in the catalyst. Moreover, as acidity increases so does the dehydration impurities.

For the three catalysts used few differences are obtained in the profile of impurities from dehydrogenation reactions vs. cyclohexanone yield, being phenol the impurity produced in higher amounts. Therefore both species Cu^+ and Cu^0 can be considered active in dehydrogenation and phenol formation.

Amounts of phenol and condensation impurities grow exponentially when reactions approach to the equilibrium suggesting that they are formed from cyclohexanone, which even explain the maximum of cyclohexanone yield observed in Fig. 4.

Although the three catalysts tested were active in cyclohexanol dehydrogenation it was noticed that higher activity was obtained with catalyst containing the smaller copper crystallite size.

Acknowledgment

This work was funded by the Spanish Ministry of Science and Innovation under contract CTM 2006-00317 and PET 2008-0130. The authors express their gratitude to UBE Corporation Europe S.A. for its support and Süd-Chemie AG by catalyst supply.

References

- [1] J. Ritz, H. Fuchs, H. Kieczka, W.C. Moran, Caprolactam, in: F.Th. Cambell, R. Pfefferkorn, J.R. Rounsaville (Eds.), Ullmann's Encyclopedia of Industrial Chemistry, vol. A5, Wiley-VCH, Weinheim, 1986, pp. 31–50.
- [2] H.A. Wittcof, B.G. Reuben, Industrial Organic Chemical, John Wiley & Sons, Inc., 1996, pp. 253–264.
- [3] G. Gut, R. Jaeger, Chem. Eng. Sci. 37 (1982) 319–326.
- [4] N.V. Nikiforova, K.A. Zhavnerko, Petrol. Chem. URSS 14 (1974) 25–31.
- [5] Y.-M. Lin, I. Wang, C.-T. Yeh, Appl. Catal. 41 (1988) 53–63.
- [6] C.H. Sivaraj, M. Reddy, B. Kanta, P. Rao, Appl. Catal. 45 (1988) L11–L14.
- [7] F.T.M. Mendes, M. Schmal, Appl. Catal. A 163 (1997) 153–164.
- [8] A. Romero, A. Santos, P. Yustos, Ind. Eng. Chem. Res. 43 (2004) 1557–1560.
- [9] D.V. Cesar, C.A. Peréz, V.M.M. Salim, M. Schmal, Appl. Catal. A 176 (1999) 205–212.
- [10] V.Z. Fridman, A.A. Davydov, J. Catal. 195 (2000) 20–30.
- [11] P. Tétényi, Z. Paál, J. Catal. 208 (2002) 494–496.
- [12] V.Z. Fridman, A.A. Davydov, J. Catal. 208 (2002) 497–498.
- [13] V.Z. Fridman, A.A. Davydov, K. Titievsky, J. Catal. 222 (2004) 545–557.
- [14] V. Siva Kumar, S. Sreevardhan Reddy, A.H. Padmasri, B. David Raju, I. Ajitkumar Reddy, K.S. Rama Rao, Catal. Commun. 8 (2007) 899–905.
- [15] D. Ji, W. Zhu, Z. Wang, G. Wang, Communication 8 (2007) 1891–1895.
- [16] B.M. Nagaraja, V. Siva Kumar, V. Shashikala, A.H. Padmasri, S. Sreevardhan Reddy, B. David Raju, K.S. Rama Rao, J. Mol. Catal. A: Chem. 223 (2004) 339–345.
- [17] B.M. Nagaraja, A.H. Padmasari, P. Seetharamulu, K. Hari Prasad Reddy, B. David Raju, K.S. Rama Rao, J. Mol. Catal. A: Chem. 278 (2007) 29–37.
- [18] K.V.R. Chary, K.K. Seela, D. Naresh, P. Ramakanth, Catal. Commun. 9 (2008) 75–81.
- [19] J.M. Campos-Martín, A. Guerrero-Ruiz, J.L.G. Fierro, J. Catal. 156 (1995) 209–212.
- [20] M.V. Twigg, Catalyst Handbook, 2nd ed., Wolfe, 1989 (Chapter 6).
- [21] Z. Wang, J. Xi, W. Wang, G. Lu, J. Mol. Catal. A: Chem. 191 (2003) 123–124.
- [22] G. Bai, X. Fan, H. Wang, J. Xu, F. He, H. Ning, Catal. Commun. 10 (2009) 2031–2035.
- [23] R.G. Herman, K. Klier, G.W. Simmons, B.P. Finn, J.B. Bulko, T.P. Kobylinski, J. Catal. 56 (1979) 407–429.
- [24] S. Menta, G.W. Simmons, K. Klier, R.G. Herman, J. Catal. 57 (1979) 339–360.
- [25] F.M. Bautista, J.M. Campelo, A. García, D. Luna, J.M. Marinas, R.A. Quirós, A.A. Romero, Appl. Catal. A Gen. 243 (2003) 93–107.
- [26] F. García-Ochoa, A. Santos, Ind. Eng. Chem. Res. 32 (1993) 2626–2632.
- [27] J.M. Rynkowski, T. Paryjczak, M. Lenik, Appl. Catal. A Gen. 106 (1993) 73–83.